

Gamma-ray signatures of classical novae

Margarita Hernanz*, Jordi Gómez-Gomar[†] and Jordi José**

**Institute for Space Studies of Catalonia (IEEC) and Instituto de Ciencias del Espacio (CSIC), Edifici Nexus, C/Gran Capità, 2-4, E-08034 Barcelona, Spain*

[†]*Institute for Space Studies of Catalonia (IEEC)*

***Institute for Space Studies of Catalonia (IEEC) and Departament de Física i Enginyeria Nuclear (UPC), Avda. Víctor Balaguer, s/n, E-08800 Vilanova i la Geltrú (Barcelona), Spain*

Abstract. The role of classical novae as potential gamma-ray emitters is reviewed, on the basis of theoretical models of the gamma-ray emission from different nova types. The interpretation of the up to now negative results of the gamma-ray observations of novae, as well as the prospects for detectability with future instruments (specially onboard INTEGRAL) are also discussed.

INTRODUCTION

Classical novae are explosive phenomena occurring in close binary systems of the cataclysmic variable type. In these binaries, a normal main sequence star overflows its Roche lobe, transferring H-rich matter to its companion white dwarf star through an accretion disk. Matter accumulates on top of the degenerate white dwarf star, where it is gradually compressed and heated, until hydrogen reaches conditions for ignition. This ignition happens in a degenerate regime, thus leading to a thermonuclear runaway, because of the inability of matter to thermally readjust itself through expansion. During explosive hydrogen burning, radioactive nuclei (with lifetimes ranging from ~ 100 s to $\sim 10^6$ s) are synthesized. The radioactive isotopes with lifetimes around 100 s, like ^{14}O ($\tau=102$ s), ^{15}O ($\tau=176$ s) and ^{17}F ($\tau=93$ s), are responsible for the explosion itself, because they can be transported by convection to the outer envelope, during the thermonuclear runaway (since $\tau_{\text{conv}} < \tau$). These nuclei are prevented from destruction in the outer cooler shells, and their subsequent decay releases energy which is largely responsible for the expansion and large increase in luminosity of the nova.

Other radioactive isotopes synthesized in novae, with longer lifetimes, are responsible for the gamma-ray emission of these objects. Two types of emission are expected: prompt emission, related with e^- - e^+ annihilation (with e^+ coming from the decay of the short-lived ^{13}N , $\tau=862$ s, and ^{18}F , $\tau=158$ min) and long-lasting emission, caused by the decay of ^7Be ($\tau=77$ days) and ^{22}Na ($\tau=3.75$ yr). The prompt emission appears very early (before optical maximum, i.e., usually before nova discovery), has short duration (a couple of days) and consists of a 511 keV line plus a continuum below it (see below for details). The long-lasting emission consists of lines (either 478 keV from ^7Be decay or 1275 keV from ^{22}Na decay), lasting around 2 months and 3 years, respectively.

The potential role of classical novae as sources of gamma-ray emission was pointed out long ago [2, 1, 20], but detailed models combining both the explosion modeling and the production and propagation of gamma-rays are more recent [10, 11, 5, 12]. Up to

now, there have been unsuccessful attempts to detect gamma-ray emission from novae. Efforts have been made mainly to detect the ^{22}Na line, at 1275 keV, with the COMPTEL instrument onboard the Compton Gamma-Ray Observatory, CGRO [14, 15]. Previous attempts to detect the ^7Be line, at 478 keV, and the 1275 keV line were made with the GRS instrument onboard the Solar Maximum Mission, SMM, satellite [6]. All these efforts have only provided upper limits, fully compatible with our theoretical predictions [18, 19].

Other attempts have concentrated on the annihilation emission (511 keV line plus continuum below it), with large field of view instruments, like WIND/TGRS [8] and CGRO/BATSE [13], without success and, again, with upper limits compatible with theoretical predictions. The possible detection of this type of emission from novae with the CGRO/BATSE instrument had been pointed out by Fishman et al. (1991) prior to CGRO launch. The sensitivities of the instruments were too low to detect the emission, which is more intense than that in the 478 and 1275 keV lines but has much shorter duration. In addition to search for gamma-ray emission in particular objects, there have been attempts to look for the Galactic accumulated emission at 478 and 1275 keV, both with CGRO/OSSE and SMM/GRS [21, 6, 7]. In this case, more flux is accumulated since more sources are contributing, because the typical period between two successive nova explosions in the Galaxy is shorter than the lifetimes of ^7Be and ^{22}Na . But again not enough sensitivity was available. We have recently made predictions about the detectability of this accumulated emission with INTEGRAL/SPI [17]; the cumulative emission around the Galactic center has some chance of being detected with SPI, during the deep survey of the central radian of the Galaxy (or, at least, better upper limits than those of SMM or COMPTEL are expected).

GAMMA-RAY EMISSION: LINES AND CONTINUUM

A summary of the main radioactive nuclei synthesized in novae is shown in table 1. It is important to stress that these nuclei are not produced in the same amounts in all the nova types, since their synthesis is closely related to the nuclear paths followed by the nova during its evolution. These paths depend on the initial chemical composition of the accreted envelope, which is related to that of the underlying white dwarf core, because some mixing between the core and the envelope should be invoked in order to explain the observed abundances of novae. It turns out that CO novae are the main producers of ^7Be , whereas ONe novae are responsible for ^{22}Na synthesis. In table 2 we show some examples of nova models, with their relevant yields of radioactive isotopes. The specific kinetic energy of the ejecta is also shown for completeness. These results have been obtained by means of a hydrodynamic code, which computes the nova evolution from the accretion phase up to the explosion and ejection of the envelope (see José & Hernanz 1998 for details). The ^{18}F yields still suffer from some uncertainty, mainly because of the not well known $^{18}\text{F}(\text{p},\alpha)$ reaction (see [3] for a recent analysis).

The gamma-ray output of a particular nova model at different epochs after the outburst (defined as the epoch of peak temperature), has been computed with a Monte Carlo code, which handles gamma-ray production and transfer in the expanding envelope (see [5] for

details), with properties derived from the hydro code models. In figure 1 we show the spectral evolution of a CO and an ONe nova ($M_{wd}=1.15$ and $1.25 M_{\odot}$, respectively), at distance 1 kpc. For all models there is a continuum between (20-30) and 511 keV, and a line at 511 keV (~ 8 keV full width half-maximum, FWHM), with intensities decreasing very fast [12]. The 511 keV line comes from the direct annihilation of positrons and from the positronium (in singlet state) emission, whereas the continuum originates in both the positronium continuum (triplet state positronium) and the Comptonization of photons emitted in the 511 keV line. There is a cutoff of the continuum at low energies (20-30 keV, depending on the chemical composition), related to photoelectric absorption, which acts as a sink of the Comptonized photons. In addition to this prompt and short-duration emission, there is a longer duration gamma-ray output, consisting of a line at 478 keV ($\sim(3-8)$ keV FWHM), in CO novae, or at 1275 keV (~ 20 keV FWHM), in ONe novae. The general trends for other CO and ONe models are similar to those shown here. It is worth noticing that models with lower masses are more opaque (i.e., the $0.8 M_{\odot}$ CO nova), because of the smaller expansion velocities (see table 2).

The light curves for the different types of emission are shown in figures 2, 3, 4 and 5. Figure 2 shows the light curve of the 511 keV line (FWHM between 3 and 8 keV) for all models, and those of different energy bands in the continuum, for an ONe nova. The continuum emission at energies lower than 511 keV dominates, being the band between 20 and 250 keV the one with the highest flux (but also the one which decreases faster, as can also be seen in figure 1). This prompt emission gives a direct insight of the dynamics of the expanding envelope, as well as information about its content on the radioactive nuclei ^{13}N and ^{18}F . In the case of ONe novae, there is also the contribution of positrons from ^{22}Na decay, which produces smaller fluxes but lasts a longer time (up to complete transparency of the envelope, which occurs at around 1 week after peak temperature, the exact value depending on the expansion velocities of the envelope).

We have analyzed the influence of the mass and the velocity of the ejecta on the prompt emission, by means of some extra models, in which we scale either the mass of the ejecta or its terminal velocity. These are in some way not self-consistent models, because they are not the result of evolutionary calculations, but they are good for illustrative purposes. Figure 3 shows the 511 keV line light curves for a CO and an ONe nova (both of $1.15 M_{\odot}$), for a range of parametrized ejected masses (the value obtained in the evolutionary model is shown in table 2). The effect of increasing the ejected mass is twofold, depending on the epoch. At early times, the larger the mass the lower the flux, because of the increasing opacity. On the contrary, later on the opacity doesn't play an important role, and the larger the mass the larger the flux, because of the larger amount of radioactive isotopes. It is worth reminding that in ONe novae the emission lasts longer than in CO ones (see figure 3, right), because of the contribution of the e^+ from ^{22}Na decay.

The influence of the velocity of the ejecta is shown in figure 4. At early times, larger velocities imply larger transparency and thus larger fluxes (both for CO and ONe novae). At later times (after ~ 2 days), only the case of ONe novae is relevant, since there are still e^+ from ^{22}Na decay; then, the larger the velocity the earlier the flux disappears, because the envelope becomes transparent before, thus allowing e^+ to freely escape (see figure 4, right). This fact demonstrates again that the analysis of the prompt gamma-ray emission of classical novae would provide a great deal of information about the dynamics of the

expanding envelope, as well as about the ratio between its ^{18}F and ^{22}Na contents.

In figure 5 we display the light curves of the 478 keV line, for the two CO novae from table 2, and those of the 1275 keV line, for the ONe novae in table 2. These light curves show a first phase of increasing flux, related to the increasing transparency of the envelope, followed by the characteristic exponential decay phase, when the envelope is already transparent. The light curve of the 478 keV line shows in addition an intense peak at early times, which comes from the Comptonization of the 511 keV photons (see above). The fluxes of the 478 and 1275 keV lines during the exponential decay phase, directly reflect the amount of ^{22}Na and ^{7}Be in the envelope.

PROSPECTS FOR DETECTABILITY OF INDIVIDUAL NOVAE

In order to predict detectability distances of the gamma-ray emission from novae, the abovementioned light curves for the different types of emission have been used. The fluxes are quite small, leading to detectability distances with INTEGRAL/SPI of around 1 kpc, for the 1275 keV line, and 0.5 kpc, for the 478 keV line, for the nominal observation time of 10^6 s (see table 3 for exact values). Concerning the 511 keV line and the continuum, detectability distances with SPI are around 3 kpc (see table 3), adopting 10 h of observation time, starting 5 h after peak temperature. For the continuum we have adopted the range (170-470) keV, which is optimal for SPI, since it avoids the 478 keV line and the low energies, where the background is too high. The width of the lines has been fully taken into account to derive all the detectability distances. As it is known, the instrument INTEGRAL/SPI will have a very good spectral resolution, which means that its nominal sensitivity for narrow lines is degraded when they are broad.

Our time origin in the figures is at peak temperature, which happens before the maximum in visual luminosity. The time interval between peak temperature and maximum in visual luminosity depends on the particular nova model, mainly on its speed class (rate of decline of the visual luminosity). It ranges from some days to some weeks, but its exact value is difficult to establish, because novae are usually discovered at or after visual maximum. Therefore, the epoch of peak temperature is close to peak gamma-ray luminosity (corresponding to the $e^- - e^+$ annihilation emission), but it is not reachable from visual observations. The early appearance, before optical detection, of the prompt gamma-ray emission from novae, makes its detection with SPI problematic. It will be only possible if a close enough nova falls in the field of view of the instrument when it is doing another observation (i.e., during the Galactic plane survey -GPS- or during the Galactic center deep exposure -GCDE). We have also considered alternative ways to detect this intense emission, by means of the SPI shield, which provides a large detection area with a wide field of view, but without spectroscopic capability [16]. In summary, the prompt gamma-ray $e^- - e^+$ annihilation emission can almost only be detected with wide field of view instruments scanning all the sky very often (like the future EXIST, MEGA, Advanced Compton Telescope). Up to now, “a posteriori” analyses (provided that there was some observation of the right field at the right moment) of the CGRO/BATSE [13] and WIND/TGRS [8] data have been performed; the negative results are fully compatible with our theoretical predictions and are related to the not enough sensitivity of these

instruments.

DISCUSSION

The main factor affecting detectability of novae is distance (see table 3), but the distances of novae are not easy to determine accurately. The visual luminosity (i.e., the absolute visual magnitude) of a classical nova at maximum is not directly correlated with its amount of the radioactive nucleus ^{22}Na , or any other radioactive nucleus (in contrast with SNIa, where ^{56}Ni is responsible for both the visual and the gamma-ray luminosities at early times). Therefore, some other characteristic, such as apparent visual magnitude, should be used as distance indicator. But, as with any cosmic object, novae which are apparently bright visually can be farther away than novae which are dim, if the visual extinction (intrinsic plus interstellar) of the apparently bright object is much smaller than that of the apparently dim object. Once the preliminary visual light curve and visual extinction are obtained, a distance determination is possible through indirect methods, which suffer from large uncertainties. They depend on various not well known nova properties. First, the empirical relationship between absolute magnitude at maximum, M_V^{\max} , and speed class of the nova (MMRD relation); the speed class is measured by the time of decline of the visual magnitude by 2 or 3 magnitudes (t_2 or t_3). Second, the visual extinction of the nova, A_V , which has intrinsic plus interstellar contributions; the latter varies a lot depending on the location of the nova in the Galaxy.

Once M_V^{\max} and A_V are known, the derivation of the distance from the apparent magnitude at maximum, m_V^{\max} , is straightforward. Therefore, the main uncertainties affecting distance determinations are: general validity of the empirical M_V^{\max} - t_2 (or t_3) relationship, determination of A_V , in addition to the determination of t_2 (or t_3) and of m_V^{\max} (often it is not known if the nova has been caught at the maximum or after it) from the observations. In figure 6, we show a m_V^{\max} -distance diagram, for novae discovered in the last century (up to 1995). The data shown are taken from the samples of Shafter [22]. We have superimposed two curves indicating the apparent magnitudes at maximum, m_V^{\max} , one could expect, provided that novae are standard candles with absolute magnitude at maximum $M_V^{\max} = -7.5$, and that visual extinction, A_V , ranges from 0 to 3 magnitudes. For distances up to 1 kpc, m_V^{\max} should be smaller (brighter) than 5.5 (for 3 kpc, m_V^{\max} ranges from 8 to 5, or brighter if M_V^{\max} is < -7.5). If we include novae after 1995, two outstanding points at $m_V^{\max} = 2.8$ and 4, and $d \sim 2$ and 4 kpc (Nova Vel 1999 and Nova Aql 1999b, respectively) would appear (with $M_V^{\max} < -7.5$; Nova Vel 1999 probably had $M_V^{\max} \sim -8.7$ (IAUC 7193)), in addition to more “normal” points with distances larger than 5 kpc and m_V^{\max} larger than 8. The number of novae discovered during the period 1991-1995 versus m_V^{\max} is also shown in figure 6.

In order to estimate the probability of having a nova at a particular distance, it is instructive to look at figure 7, which shows an histogram of the novae distances for the same nova set mentioned above [22], as well as for the subset of novae in the 1991-1995 period. The sample of years 1991-1995 suffers from small number statistics, but it is more representative of recent more accurate observations. Although the distances have a large uncertainty, some general trends can be extracted: the observed nova rate for

novae at distances shorter than 1 kpc is $1/5=0.20 \text{ yr}^{-1}$ (1991-1995 set), or $16/95=0.17 \text{ yr}^{-1}$ (complete set 1901-1995), which is not very large. If we relax the distances of detectability of novae by INTEGRAL by a factor of 3 (i.e., we adopt 3 kpc instead of 1 kpc, invoking the effect of the uncertain ejected masses -for some observed novae- by a factor of 10), the observed nova rate increases to $6/5=1.20 \text{ yr}^{-1}$ (1991-1995 nova set), or $50/95=0.53 \text{ yr}^{-1}$ (complete set 1901-1995). Therefore, there is some chance to have a close nova during INTEGRAL's lifetime (2 to 5 years).

Concerning future instrumentation, if an increase of sensitivity by a factor of 10 (for broad lines) is achieved, the detection of novae would be a routine instead of a chance. If, in addition, these instruments have wide fields of view and are designed to perform frequent surveys of the sky in the hard X-ray domain ($E>100 \text{ keV}$), then the prompt e^-e^+ annihilation gamma-ray emission of novae could be detected for many Galactic novae. This fact would be crucial not only for the understanding of the nova explosion mechanism itself, but also for the knowledge of the nova distribution in the Galaxy ([9]. This distribution is not at all known, since only 3-5 of the 35 ± 11 Galactic novae exploding every year are discovered optically nowadays.

REFERENCES

1. Clayton D.D., 1981, ApJ, 244, L97
2. Clayton D.D., Hoyle F., 1974, ApJ, 187, L101
3. Coc A., Hernanz M., José J., Thibaud J.P., 2000, A&A, 357, 561
4. Fishman G.J. et al., 1991, in Durouchoux P., Prantzos N., eds., Gamma-Ray Line Astrophysics. AIP, New York, p. 190
5. Gómez-Gomar J., Hernanz M., José J., Isern J., 1998, MNRAS, 296, 913
6. Harris M.J., Leising M.D., Share G.H., 1991, ApJ, 375, 216
7. Harris M.J., et al. 1996, A&AS, 120, 343
8. Harris M.J., et al. 1999, ApJ, 522, 424
9. Harris M.J., et al. 2000, ApJ, 542, 1057
10. Hernanz M., Gómez-Gomar J., José J., Isern J., 1997a, in 2nd INTEGRAL Workshop "The transparent Universe". ESA SP-382, Noordwijk, p. 47
11. Hernanz M., Gómez-Gomar J., José J., Isern J., 1997b, in 4th COMPTON Symposium. AIP, New York, 1125
12. Hernanz M., José J., Coc A., Gómez-Gomar J., Isern J., 1999, ApJ, 526, L97
13. Hernanz M., Smith D.M., Fishman J., Harmon A., Gómez-Gomar J., José J., Isern J., Jean P., 2000, in 5th COMPTON Symposium. AIP, New York, 82
14. Iyudin A.F., et al. 1995, A&A, 300, 422
15. Iyudin A.F., et al. 1999, Astrophys. Lett. & Comm., 38, 371
16. Jean P., Gómez-Gomar J., Hernanz M., José J., Isern J., Vedrenne G., Mandrou P., Schönfelder V., Lichten G., Georgii R., 1999, Astrophys. Lett. & Comm., 38, 421
17. Jean P., Hernanz M., Gómez-Gomar J., José J., 2000, MNRAS, 319, 350
18. José J., Hernanz M., 1998, ApJ, 494, 680
19. José J., Coc A. & Hernanz M. 1999, ApJ, 520, 347
20. Leising M.D., Clayton D., 1987, ApJ, 323, 159
21. Leising M.D., Share G.H., Chupp E.L., Kanbach G., 1988, ApJ, 328, 755
22. Shafter A.W. 1997, ApJ, 487, 226
23. Starrfield S., Truran J.W., Wiescher M.C., Sparks W.M. 1998, MNRAS, 296, 502

TABLE 1. Radioactive isotopes ejected by novae relevant for gamma-ray emission

Isotope	Lifetime	Main disintegration process	Type of γ -ray emission	Nova type
^{13}N	862 s	β^+ -decay	511 keV line & continuum	CO and ONe
^{18}F	158 min	β^+ -decay	511 keV line & continuum	CO and ONe
^7Be	77 days	e^- -capture	478 keV line	CO
^{22}Na	3.75 years	β^+ -decay	1275 keV & 511 keV lines	ONe
^{26}Al	10^6 years	β^+ -decay	1809 keV & 511 keV lines	ONe

TABLE 2. Radioactivities in novae ejecta (^{13}N and ^{18}F at 1h after T_{peak})

Nova	$M_{wd}(\text{M}_\odot)$	$M_{ejec}(\text{M}_\odot)$	KE (erg/g)	$^{13}\text{N} (\text{M}_\odot)$	$^{18}\text{F} (\text{M}_\odot)$	$^7\text{Be} (\text{M}_\odot)$	$^{22}\text{Na} (\text{M}_\odot)$
CO	0.8	6.2×10^{-5}	8×10^{15}	1.5×10^{-7}	1.8×10^{-9}	6.0×10^{-11}	7.4×10^{-11}
CO	1.15	1.3×10^{-5}	4×10^{16}	2.3×10^{-8}	2.6×10^{-9}	1.1×10^{-10}	1.1×10^{-11}
ONe	1.15	2.6×10^{-5}	3×10^{16}	2.9×10^{-8}	5.9×10^{-9}	1.6×10^{-11}	6.4×10^{-9}
ONe	1.25	1.8×10^{-5}	4×10^{16}	3.8×10^{-8}	4.5×10^{-9}	1.2×10^{-11}	5.9×10^{-9}

TABLE 3. SPI 3σ detectability distances (in kpc) for lines and continuum (see text for details about T_{obs}).

Nova type	$M_{wd}(\text{M}_\odot)$	511 keV line	478 keV line	1275 keV line	(170-470) keV
CO	0.8	0.7	0.4	-	0.4
CO	1.15	2.4	0.5	-	2.0
ONe	1.15	3.7	-	1.1	3.0
ONe	1.25	4.3	-	1.1	3.0

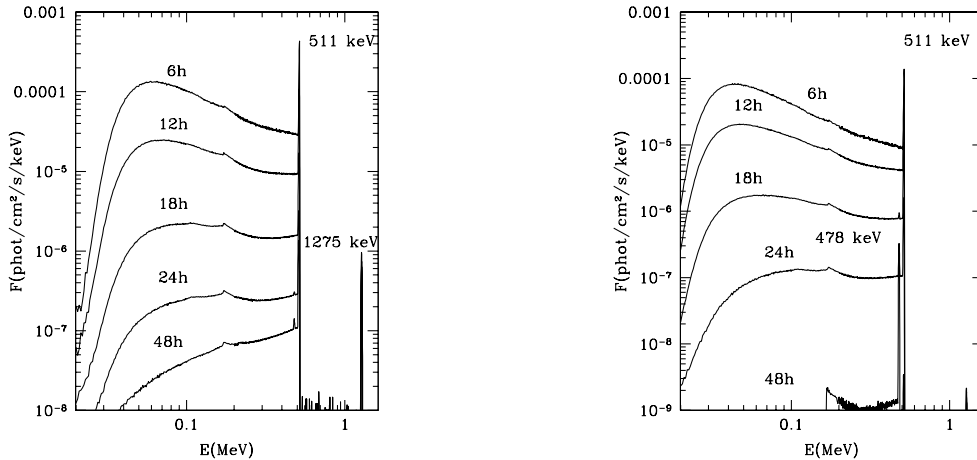


FIGURE 1. (Left) Gamma-ray spectra for an ONe nova of 1.25M_\odot , at different epochs after the outburst (defined as the peak temperature time) and at distance 1 kpc. (Right) Same for a CO nova of 1.15M_\odot

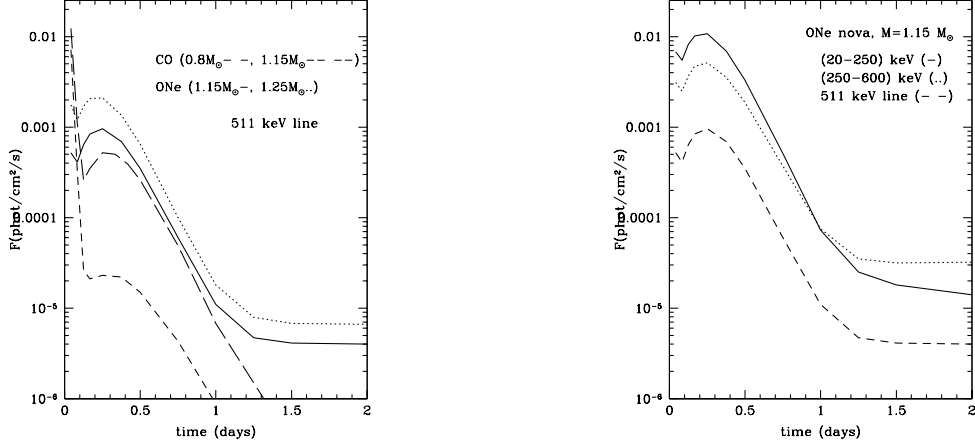


FIGURE 2. (Left) Light curves for the 511 keV line of the 4 nova models shown in table 2, placed at a distance of 1 kpc. (Right) Continuum light curves for the ONe nova of $1.15 M_{\odot}$ at the same distance.

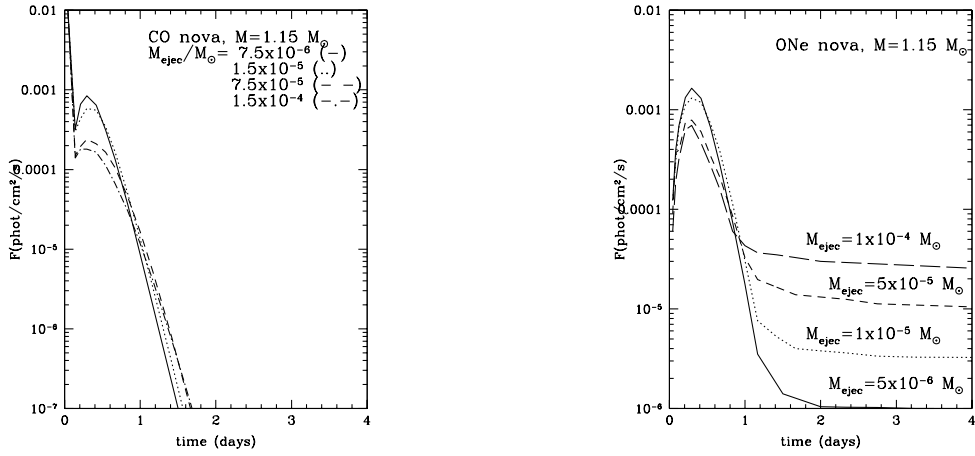


FIGURE 3. (Left) Light curves for the 511 keV line for a CO nova of $1.15 M_{\odot}$, for a range of ejected masses. (Right) Same for an ONe nova of $1.15 M_{\odot}$. Distance is 1 kpc.

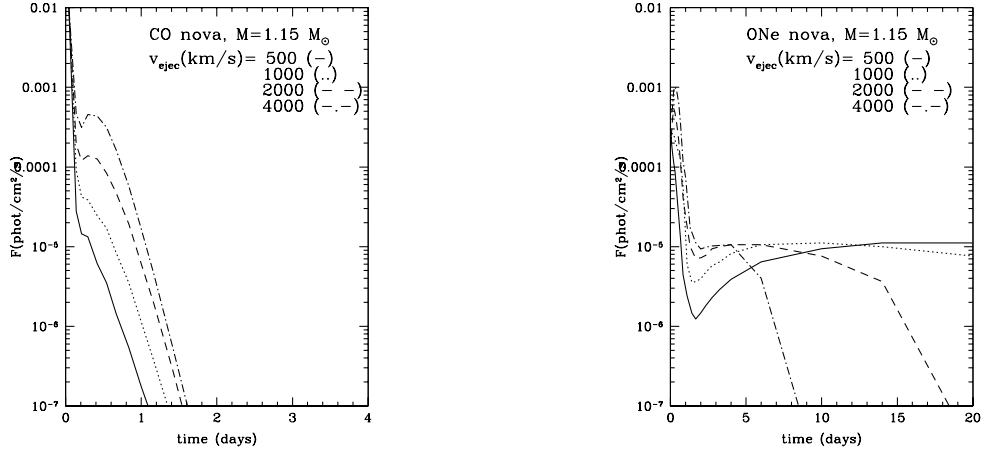


FIGURE 4. (Left) Light curves for the 511 keV line for a CO nova of $1.15 M_{\odot}$, for a range of parametrized velocities of the ejecta. The value indicated corresponds to the outermost shell. (Right) Same for an ONe nova of $1.15 M_{\odot}$. Distance is 1 kpc.

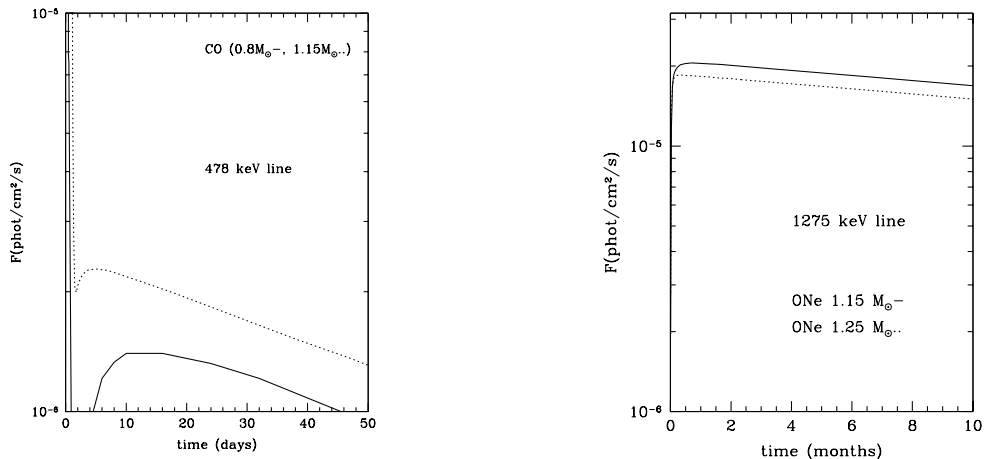


FIGURE 5. (Left) Light curves for the ^{7}Be line (478 keV) for two CO nova models. (Right) Light curves for the ^{22}Na (1275 keV) for two ONe models. Distance is 1 kpc.

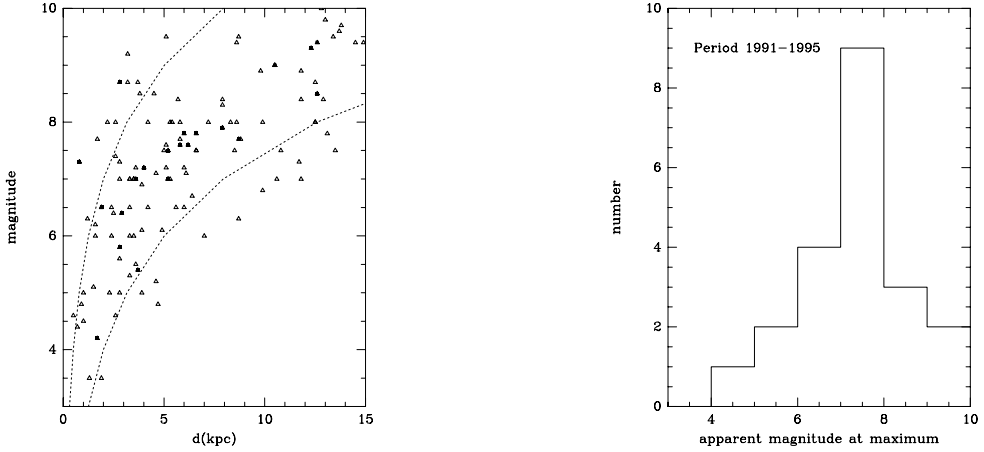


FIGURE 6. (Left) Apparent visual magnitudes at maximum, m_V^{max} , versus distances. Filled squares correspond to the 1991-1995 period and open triangles to the 1901-1990 period. The dashed curves represent the m_V^{max} vs. distance relationship obtained for an absolute $M_V^{max} = -7.5$ (typical for novae) and a range of visual extinctions (from right to left $A_V = 0$ and $A_V = 3$ magnitudes). (Right) Histogram of novae apparent magnitudes at maximum, for the novae in the period 1991-1995.

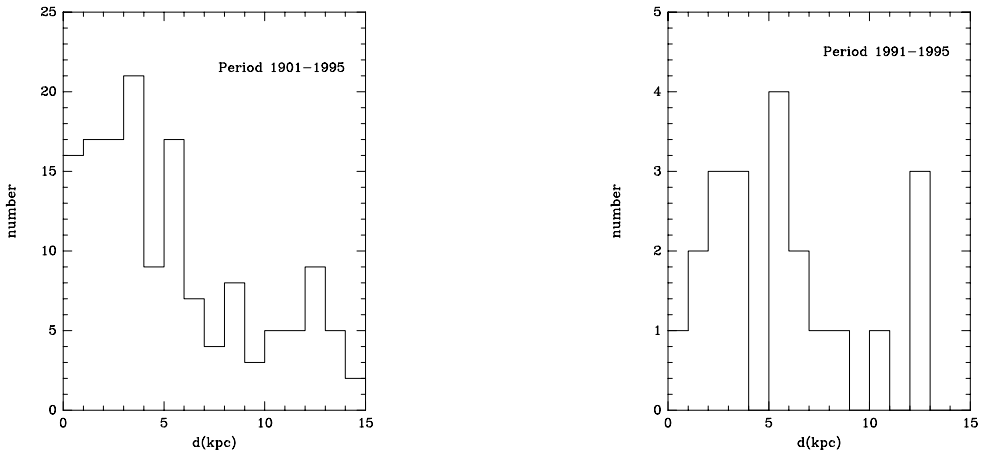


FIGURE 7. (Left) Histogram of novae distances for the novae discovered in the last century (until 1995). (Right) Same for the subset of the recent novae in the period 1991-1995